

Elsevier Editorial System(tm) for NIMB Proceedings
Manuscript Draft

Manuscript Number:

Title: Surface damage in TEM thick alpha-Fe samples by implantation with 150 keV Fe ions

Article Type: SI: NIMB_COSIRES2014

Section/Category: SI: NIMB_COSIRES2014

Keywords: Molecular dynamics; defects; Ion irradiation; Surface damage; Metals; transmission electron microscopy

Corresponding Author: Ms. Maria Jose Aliaga Gosalvez,

Corresponding Author's Institution: Universidad de Alicante

First Author: Maria Jose Aliaga Gosalvez

Order of Authors: Maria Jose Aliaga Gosalvez; Maria Jose Caturla; Robin Schaublin

Abstract: We have performed molecular dynamics simulations of implantation of 150keV Fe ions in pure bcc Fe. The thickness of the simulation box is of the same order of those used in in-situ TEM analysis of irradiated materials. We assess the effect of the implantation angle and the presence of front and back surfaces. The number and type of defects, ion range, cluster distribution and primary damage morphology are studied. Results indicate that, for the very thin samples used in in-situ TEM irradiation experiments the presence of surfaces affect dramatically the damage produced. At this particular energy, the ion has sufficiently energy to damage both the top and the back surfaces and still leave the sample through the bottom. This provides new insights on the study of radiation damage using TEM in situ.

Suggested Reviewers: Yuri Osetsky
osetskiyyn@ornl.gov

Roger Smith
R.Smith@lboro.ac.uk

COSIRES 2014

Surface damage in TEM thick α -Fe samples by implantation with 150 keV Fe ions

M. J. Aliaga^a, M. J. Caturla^a, R. Schäublin^b

*a*Dept. Física Aplicada, Facultad de Ciencias, Fase II, Universidad de Alicante, Alicante, E-03690, Spain

*b*Metal Physics and Technology, Department of Materials, ETH Zürich, HCI G515, Vladimir-Prelog-Weg 5, 8093 Zürich, Switzerland

1

2

3

4

Abstract

6

We have performed molecular dynamics simulations of implantation of 150keV Fe ions in pure bcc Fe. The thickness of the simulation box is of the same order of those used in *in-situ* TEM analysis of irradiated materials. We assess the effect of the implantation angle and the presence of front and back surfaces. The number and type of defects, ion range, cluster distribution and primary damage morphology are studied. Results indicate that, for the very thin samples used in in-situ TEM irradiation experiments the presence of surfaces affect dramatically the damage produced. At this particular energy, the ion has sufficiently energy to damage both the top and the back surfaces and still leave the sample through the bottom. This provides new insights on the study of radiation damage using TEM in situ.

14

15

Keywords: Molecular dynamics; defects; Ion irradiation; Surface damage; Metals; transmission electron microscopy

17

18

19

20

21

22

1. Introduction

24

Ion irradiation experiments are being used extensively to understand the fundamental aspects of the damage produced in metals and alloys by irradiation [1]. In the current nuclear power plants and experimental fusion reactors the damage is produced by neutrons. However, the study of neutron irradiation is difficult since conditions cannot be easily controlled, samples are activated and experiments are very costly. For this reason, ion irradiation is nowadays being used to gain basic understanding of the effects of radiation in the structural materials of the reactors.

31

32

Iron is the main element of the reactor vessel, and although it has been studied for many years, there are still many issues under debate considering its radiation damage. Both neutrons and Fe ions produce damage in cascades, but their damage profile is very different. Neutrons have a long range of penetration and produce damage quite homogeneously, whereas ion damage is more superficial. However, 100 keV Fe ions have been used in the last few years to approach indirectly the study of neutron irradiation in Fe, since the first Fe atom that is hit by a neutron in a lattice (primary knocked-on atom o PKA) has around 100 keV energy [2]. The irradiated samples can then be examined by in-situ TEM [3] in facilities such as Jannus at CEA in France [4] or the IVEM-Tandem Facility at Argonne National Laboratory [5]. Using this characterization technique the sample can be observed while it is being irradiated. The requirement is that it has to be between 40 and 100 nm thick to be transparent to electrons.

42

As it has been demonstrated in previous works [6-13] the presence of surfaces in metals affect the damage produced in the material, being quite different from the damage in bulk. Earlier, it has been observed that irradiation at room temperature of pure Fe in the form of a transmission electron microscopy (TEM) thin film leads to $a_0 < 100$ >

46

47

48

49

dislocation loops while in the bulk form irradiated Fe exhibits mainly $\frac{1}{2} a_0 \langle 111 \rangle$ [14]. This has been attributed to so-called elastic ‘image forces’ due to the free surfaces but never quantified. This effect is confirmed in recent works [15-18]. In this paper we continue our work from an atomistic point of view with the study of the primary damage produced by Fe ions of 150 keV in thin films of pure Fe using molecular dynamics.

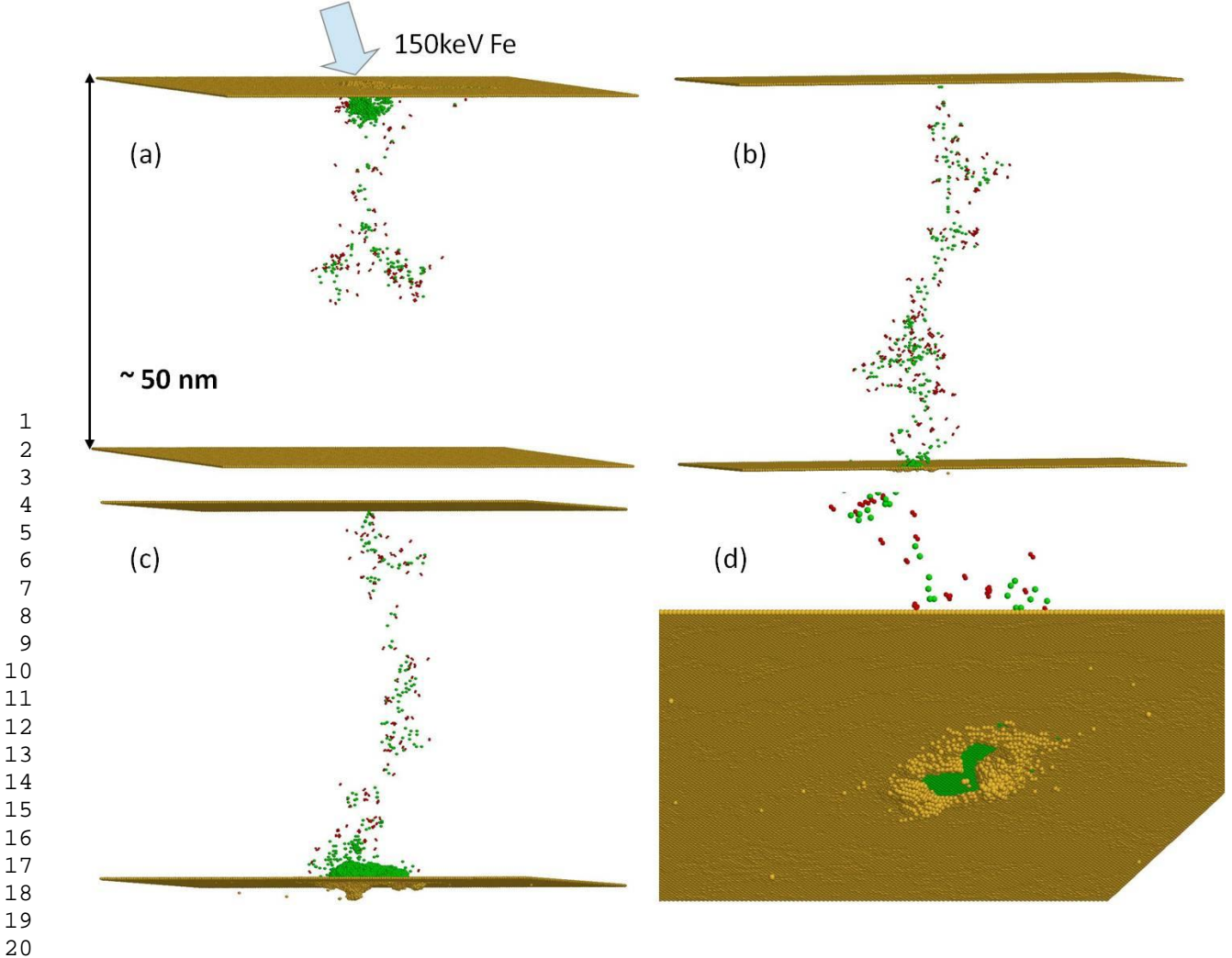
2. Methodology

Calculations were performed using the molecular dynamics code MDCASK with the interatomic potential of Dudarev and Derlet [19]. This potential was modified for short range interactions following the procedure described in [20]. Displacement cascades were simulated sending an Fe atom with an energy of 150 keV towards the top free surface of a [001] thin film of α -Fe. Two impinging angles have been used, 10° and 22° , being this second angle the one used in the TEM in situ analysis of ion irradiation experiments at Orsay JANNUS facility [4]. 20 cases were run for each angle. Variability was introduced changing the azimuthal angle from 0° to 200° . Simulation cells contained 10,076,401 atoms with a size of $180 a_0 \times 180 a_0 \times 180 a_0$, where a_0 is the lattice parameter for Fe ($a_0 = 2.8665 \text{ \AA}$). This size corresponds to thin films of about 50 nm. The setup described corresponds to the energies used in the experiments for low doses of Yao et al. [15].

Temperature was kept close to 0 K in order to avoid thermal vibrations and thus facilitate the identification of defects. The excess energy deposited by the injected atom is dissipated by adding a thermal bath that scales the velocity of two atom layers at the border of the simulation cell. Inelastic energy losses were included by the Lindhard model [21], which introduces a friction force proportional to the velocity. This force was introduced only for those atoms with a kinetic energy larger than 5 eV. Periodic boundary conditions are imposed in two axes, while free surfaces are considered in the third axis. Simulations were run until the number of defects reached a stable population (25 picoseconds in most cases). Wigner-Seitz cells were used to identify the defects. Then the defects are grouped in clusters considering that two defects belong to the same cluster when the distance between them is between first and second nearest neighbours.

3. Results

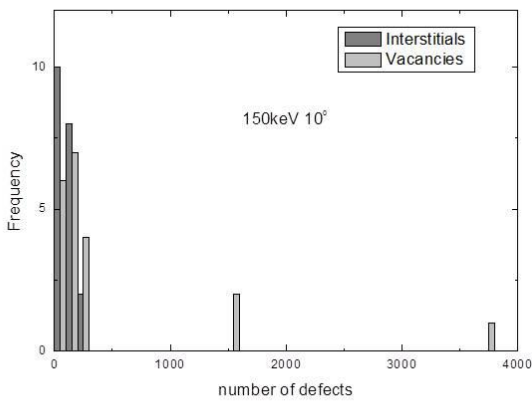
Figure 1 shows the primary damage of three representative cases of the events found in the simulations after the irradiation with a 150 keV Fe atom. The location of vacancies (light circles) and self-interstitials (dark circles) are shown for the three cases after the simulation had run for 25 ps. The arrow indicates approximately the initial position of the energetic atom. Both surfaces and adatoms are also represented in the figure. In Figure 1(a) the Fe atom is launched with an angle of 10° impacting heavily and depositing most of its energy near the top surface. The damage is divided into 3 displacement subcascades. The first and most energetic one occurs at the surface, creating a large vacancy cluster of 1070 vacancies, another vacancy cluster of 115 vacancies and 493 adatoms and 764 sputtered atoms (not shown in the figure) above the surface. The other two subcascades are around the centre of the simulation cell where the ion stops. The total number of vacancies is 1557 and the total number of interstitials is 155. In Figure 1(b) the Fe atom is sent with an angle of 22° and travels through the whole sample leaving the film at the bottom surface with 20% of its initial energy, so depositing 80% of the total 150 keV energy. In this case both top and bottom surfaces are damaged, but the back surface more strongly, with the creation of a 196 vacancy cluster. Finally Figure 1(c) shows an event in which the atom impinges with a 10° angle and again goes through the entire sample, but in this case it stops just before it escapes the film due to a strong collision with the back surface. In this case the top surface barely suffers any damage, but in the bottom surface a huge crater of 3441 vacancies is created, as well as large islands of adatoms. Figure 1(d) shows a close-up of the crater created at the bottom surface of the case represented in Figure 1(c).



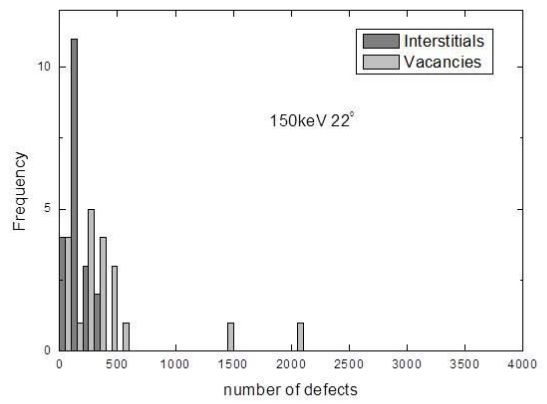
1
 2
 3
 4
 5
 6
 7
 8
 9
 10
 11
 12
 13
 14
 15
 16
 17
 18
 19
 20
 21 Fig. 1. Figures from (a-c) show three representative 150 keV cascades of Fe implantation in Fe after 25 ps. Light circles are
 22 vacancies and darker circles are interstitials. Both surfaces are also represented. The arrow indicates the implanted Fe atom. In (a)
 23 and (c) the Fe atom impact angle is 10° and in (b) the impact angle is 22° off normal. In (d) a close-up of the bottom surface
 24 damage produced in (c) is shown.

25
 26
 27 Figure 2 represents the histograms of the total number of vacancies and interstitials that results from the 20 cases
 28 simulated for an impact angle of 10° (two of these cases shown in figures 2(a) and 2(c)) and the other 20 cases for
 29 the impact angle of 22° (one example in figure 2(b)). As already shown in previous works [6,12] the number of
 30 vacancies for cascades with near surfaces is greater than the number of self-interstitials. This is due to the attraction
 31 the self-interstitials suffer by the surface. Also, the dispersion of results is larger than in bulk cascades. The main
 32 difference with [6] for the same energy is that the increase in the angle results in some events (3 for 10° and 2 for
 33 22°) with a huge number of vacancies. Two of these events for the impact angle of 10° are the ones represented in
 34 Figure 1(a) and 1(c). These type of events correspond to cases where the energetic Fe atom injected has a strong
 35 collision near the top or the back surface.

36
 37
 38
 39
 40
 41
 42
 43
 44
 45
 46
 47
 48
 49



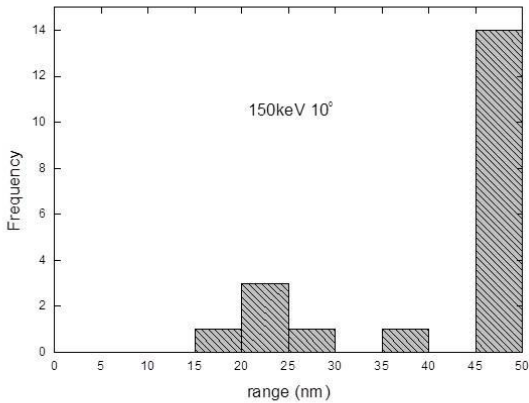
(a)



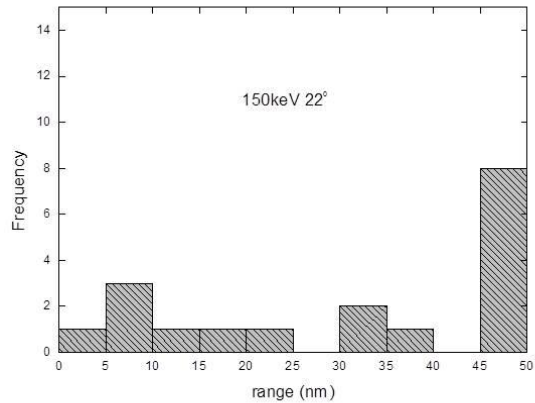
(b)

Fig. 2. Defect distribution for a series of 20 simulations of cascades in thin films produced by irradiation with a 150 keV Fe atom impacting with an angle of (a) 10° and (b) 22° of the normal.

The histograms of the ion ranges for both angles are presented in figure 3. Comparing both angles it is clear, on one hand, that in the majority of cases the PKA has enough energy to escape the sample through the bottom surface, and, on the other hand, that an increase in the impact angle from 10° to 22° leads to a reduction in the ion range, as expected. As with the number of defects, there is a wide spread in the results for the different cases. The cases where the ion range is very short coincide usually with the cases where the Fe atom has collided very strongly with or near the top surface. Indeed, in one of the two events for 22° with many vacancies, 1441 in this case, the PKA is backscattered after colliding with an atom near the top surface, creating a large $\langle 100 \rangle$ loop with 521 vacancies. On average, the energy deposited for 10° impacts is 67%, and 86% for 22° .



(a)



(b)

Fig. 3. Statistical analysis of ion ranges for the 150 keV Fe atom impacting with an angle of (a) 10° and (b) 22° of the normal.

Table 1 summarizes the mean values obtained from fitting the above histograms for the number of vacancies, self-interstitials and the ion range to either lognormal or Gaussian distributions. The percentage of vacancies and

self-interstitials in clusters and in large clusters (more than 55 defects) are also shown. It can be seen on the table, as mentioned above, that the ion range for 22° with a value of 30 nm is shorter than the value for 10° which is 42 nm. The SRIM values [22] are 50 nm for the ion range at an impact angle of 10° and 47 nm for the ion range at an impact angle of 22°. This is reasonable because SRIM assumes on one hand a random target, and on the other hand these events where the ion interacts very energetically with the surfaces shortening its range do not happen.

Table 1 Average number of vacancies and interstitials and their cluster fractions after the 150 keV cascades. Large clusters contain more than 55 defects. The ion range is also shown.

Angle (°)	Number of vacancies	Number of interstitials	% V in clusters	% V in large clusters	% I in clusters	% I in large clusters	Ion range (nm)
10	132	73	43	12	24	0	42
22	225	166	47	16	27	0	30

The increase in the angle also has an effect, as expected, on the mean value of vacancies and interstitials. The angle of 10° is still slightly below the Lindhard critical angle for channeling [23] which, for 150 keV is 12° and this results in a lower number of defects as a mean value. Figure 4 represents the distribution of clusters normalized by the number of cascades for both angles. It can be seen a tendency to larger clusters of vacancies and interstitials from 10° to 22°, but this increase is not remarkable because at 10° there are events where the back surface is profoundly damaged.

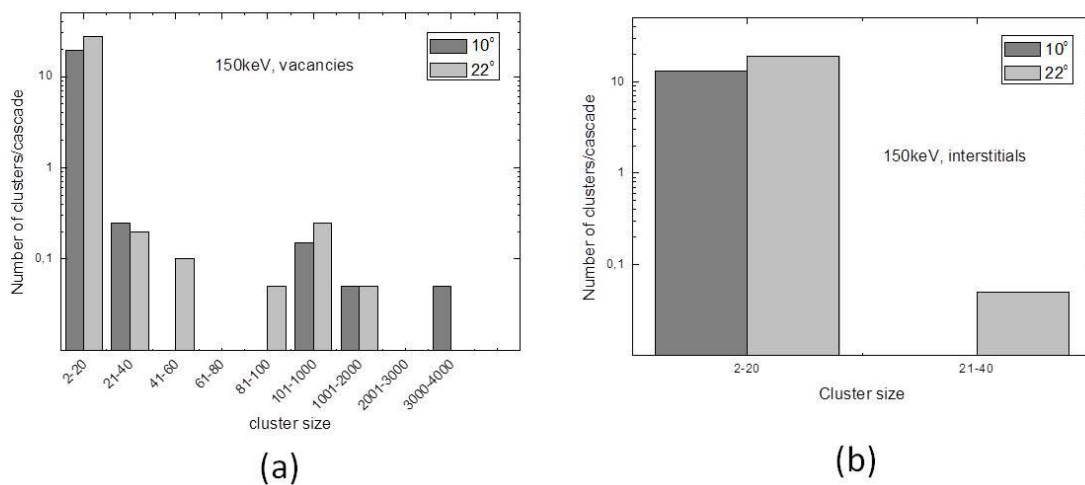


Fig. 4. Histograms of number of vacancy (a) and interstitial (b) clusters of different sizes normalized to the number of cascades.

4. Conclusions

The primary damage produced in thin films of pure bcc Fe by irradiation with 150 keV Fe ions using two different implantation angles has been studied. Results show that, differently from lower energies where only the top surface is quite affected, at this energy regime front and back surfaces can be damaged. When the ion impacts strongly with or near one of the surfaces the creation of large vacancy clusters is observed. This is produced by the attraction the self-interstitials suffers when they are close enough to the surface. These results have important implications for higher energies, because they indicate that at high irradiation energies, like the range of energies used mainly in the in-situ TEM irradiation experiments, the damage will be produced mostly at the back surface of the film. Moreover, these effects should be taken into account in models that predict the latter evolution of damage and damage accumulation, such as kinetic Monte Carlo or rate theory calculations.

These calculations provide new insights on the study of radiation damage using TEM in situ irradiation experiments, providing the fundamental background needed to use the data from TEM in situ experiments to understand damage in bulk specimens.

Acknowledgements

We would like to thank Drs. R. Schaublin, A. Prokoldtseva, M. Hernández-Mayoral, Z. Yao and S. Dudarev for fruitful discussions. Simulations were carried out in the computer cluster of the Dept. of Applied Physics at the UA, the HPC-FF supercomputer of the Jülich Supercomputer Center, Germany, and the HELIOS supercomputer in Japan. MJA thanks the UA for support through an institutional fellowship. This work was supported by the European Fusion Development Agreement (EFDA), the VII EC framework through the GETMAT and MATISSE projects, and the Generalitat Valenciana PROMETEO2012/011.

References

- [1] J.L. Boutard, A. Alamo, R. Lindau, M. Rieth, 2008 *C. R. Phys.* **9** 287
- [2] Hernández Mayoral, Mercedes. Estudio por Microscopía Electrónica de Transmisión del efecto de la irradiación iónica y neutrónica en hierro puro y aleaciones modelo de los aceros de vasija de los reactores nucleares. Madrid, 2007. Centro de Investigaciones energéticas, Medioambientales y Tecnológicas (CIEMAT). Departamento de Tecnología, División de Materiales.
- [3] Y. Matsukawa, S. J. Zinkle, 2007 *Science* **318** 959
- [4] <http://jannus.in2p3.fr/spip.php?rubrique15>.

- [5] C.W. Allen, L.L. Funk, E.A. Ryan, 1996 *Mat. Res. Soc. Symp. Proc.* **396** 641.
- [6] M.J. Aliaga, A. Prokhotseva, R. Schaeublin, M.J. Caturla, *Journal of Nuclear Materials* 452 (2014) 453-456.
- [7] M. Ghaly, R.S. Averback, *Phys. Rev. Lett.* 72 (1994) 364.
- [8] K. Nordlund, J. Keinonen, M. Ghaly, R.S. Averback, *Nature* 398 (1999) 48.
- [9] K. Nordlund, J. Keinonen, M. Ghaly, R.S. Averback, *Nucl. Instr. And Meth. In Phys. Res. B* 148 (1999) 74-82.
- [10] S. V. Starikov, Z. Insepov and J. Rest , *Phys. Rev. B* 84, 104109 (2011)
- [11] P.D. Lane, G. J. Galloway, R. J. Cole, M. Caffio, R. Schaub, G. J. Ackland., *Phys. Rev. B* 85, 094111 (2012).
- [12] R. E. Stoller, *J. Nucl. Mater.* 307-311 (2002) 935.
- [13] R. E. Stoller, S. G. Guiriec, *J. Nucl. Mater.* 329 (2004) 1238.
- [14] Masters B. *Nature* 1963; 200:254
- 1 [15] Z. Yao, M. Hernández Mayoral, M. L. Jenkins, M. A. Kirk, *Phil. Mag.* 88 (2008) 2851.
- 2 [16] M. Hernández Mayoral, Z. Yao, M. L. Jenkins, M. A. Kirk, *Phil. Mag.* 88 (2008) 2881.
- 3 [17] A. Prokhotseva, B. Décamps, R. Schäublin, 2013 *J. of Nucl. Mat.* **442** S786-S789
- 4 [18] A. Prokhotseva, B. Décamps, A. Ramar, R. Schäublin, 2013 *Acta Materialia* 61 (2013) 6958-6971.
- 5 [19] S. Dudarev, P. Derlet, *J. Phys. Condens. Matter.* 17 (2005) 1-22.
- 6 [20] C. Björkas, K. Nordlund, *Nucl. Instrum. Methods Phys. Res. B* 259 (2007) 853-860.
- 7 [21] J. Lindhard and M. Sharff, *Phys. Rev.* 124, 128 (1961).
- 8 [22] J. F. Ziegler, J. P. Biersack, *The Stopping and Range of Ions in Matter*, SRIM-2003, Ó1998, 1999 by IB77M co.
- 9 [23] L.P. Zheng., Zhi-Yuan Zhu, Yong Li, Frank O. Goodman, *Nucl. Instrum. Methods Phys. Res. B* 268 (2010) 120-122.
- 10
- 11
- 12
- 13
- 14
- 15
- 16
- 17
- 18
- 19
- 20
- 21
- 22
- 23
- 24
- 25
- 26
- 27
- 28
- 29
- 30
- 31
- 32
- 33
- 34
- 35
- 36
- 37
- 38
- 39
- 40
- 41
- 42
- 43
- 44
- 45
- 46
- 47
- 48
- 49

1
2
3
4
5
6
7
8
9
10
11
12
13
14
15
16
17
18
19
20
21
22
23
24
25
26
27
28
29
30
31
32
33
34
35
36
37
38
39
40
41
42
43
44
45
46
47
48
49